2

SAND91-0031C

Conf-9108110--1

LEAD-FREE SOLDERS FOR ELECTRONICS APPLICATIONS: WETTING ANALYSIS

SAND--91-0031C

DE91 014900

P. T. Vianco, F. M. Hosking, D. R. Frear
Metallurgy Department
Sandia National Laboratories
Albuquerque, NM 87185

1991

ABSTRACT

The fabrication of electronic systems has relied upon eutectic tin-lead solder for the attachment of components to printed wiring boards. Higher service temperatures are approaching the durability limits of the eutectic solder. The tin-rich, lead-free solders are being actively studied as alternate alloys. Experiments that examined the wettability of 95Sn-5Sb (wt.%), 95.5Sn-4.0Cu-0.5Ag, 96.5Sn-3.5Ag, and the control solder, 60Sn-40Pb, on oxygen-free, high conductivity copper were performed. A rosin-based, mildly activated (RMA) flux and three water soluble, organic acid fluxes were used in the wetting balance/meniscometer measurements. The 95.5Sn-4.0Cu-0.5Ag and 95Sn-5Sb alloys exhibited good wetting, with contact angles of $35° < \theta_c < 55°$ as compared to the excellent performance of the 60Sn-40Pb material ($20° < \theta_c < 35°$). The fair wettability observed with the 96.5Sn-3.5Ag solder ($60° < \theta_c < 75°$) was due in large part to the inability of the fluxes to significantly lower the solder-flux interfacial tension. The wetting rates of the 95.5Sn-4.0Cu-0.5Ag and 95Sn-5Sb solders were comparable to those of the control; the 96.5Sn-3.5Ag alloy wetting rate was slower than the other candidates. The solder film formed on the substrate surface by the 95.5Sn-4.0Cu-0.5Ag alloy was very grainy. The water soluble fluxes exhibited a larger degree of residue formation than did the RMA flux.

INTRODUCTION

THE EUTECTIC TIN-LEAD ALLOY, 63Sn-37Pb (wt.%), remains the dominant solder used for component attachment in electronic systems. However, customers and designers are requiring higher service temperatures for their printed wiring board (PWB) assemblies. This trend has resulted in substantial improvements to the elevated temperature performance of PWB materials. However, it must be recognized that the harsher operating conditions are approaching the practical limits of 63Sn-37Pb solder. Alternative solders have been principally the lead-rich alloys: e.g., 10Sn-90Pb and 5Sn-95Pb with liquidus temperatures of 305°C and 315°C, respectively. These temperatures, coupled with the added 40°C margin for the actual working temperature, tax the robustness of the PWB material. Vianco and Dal Porto [1] observed damage to polyimide-quartz PWB substrates and a weakening of the solder pad-substrate bond when the 10Sn-90Pb alloy was used to hand-solder edge clips to polyimide quartz circuit boards. Automated soldering is also made difficult by the working temperatures of these solders.

At melting temperatures intermediate to the 63Sn-37Pb alloy and the lead-rich solders are the tin-rich, lead-free solders: 95.5Sn-4.0Cu-0.5Ag [2] (T_s=216°C, T_l=222°C); 96.5Sn-3.5Ag (T_s=T_l=221°C); and 95Sn-5Sb (T_s=232°C, T_l=240°C). The use of pure tin was discouraged because of (1) low hardness and resistance to deformation [3], (2) the low temperature (13°C) transformation of white to gray tin, and (3) the growth of tin whiskers in ambient environments. The tin-rich, lead-free alloys are typically thought of as plumbing solders and so have not received a great deal of study for electronic applications.

An extensive effort is under way to investigate (1) the wettability, (2) the solderability of structural and electronic joints, and (3) the elevated temperature aging of the microstructure and solder-substrate intermetallic layers of the tin-rich, lead-free solders. The wettability study, which is highlighted here, was designed to evaluate these solders with the customary rosin-based, mildly activated (RMA) flux and with three water soluble, organic acid (OA) fluxes. The OA fluxes were examined in response to regulations restricting the future use of cleaning solvents [4] required to remove the residues left by the RMA flux. Adequate wettability is the first step toward achieving successful solderability of particular components and PWB assemblies.

EXPERIMENTAL PROCEDURES

PROCEDURES – Wettability was assessed quantitatively by the contact angle, θ_c, formed at the edge of a solder meniscus on the sample coupon immersed into a solder bath (Fig. 1). The contact angle, which is defined by Young's equation given at the bottom of Fig. 1, acts as a generalized parameter to describe the equilibrium conditions between the solder(L)-substrate(S) interfacial tension, γ_{SL}; the substrate(S)-flux(F) interfacial tension, γ_{SF}; and the solder(L)-flux(F) interfacial tension, γ_{LF}. *Wettability is optimized by the smallest possible value of the contact angle.* The lowest value of θ_c is realized by a minimum value of γ_{LF}, a large value of γ_{SF} (oxide- and contaminant-free sample surfaces) and a small value of γ_{SL} (strong metallurgical interactions between the solder and the substrate). The parameters θ_c and γ_{LF} were calculated from mathematical expressions based upon two experimentally measured properties of the meniscus: the meniscus height, H and the meniscus weight, W (Fig. 2).

DISCLAIMER

This report was prepared as an account of work sponsored by an agency of the United States Government. Neither the United States Government nor any agency thereof, nor any of their employees, makes any warranty, express or implied, or assumes any legal liability or responsibility for the accuracy, completeness, or usefulness of any information, apparatus, product, or process disclosed, or represents that its use would not infringe privately owned rights. Reference herein to any specific commercial product, process, or service by trade name, trademark, manufacturer, or otherwise does not necessarily constitute or imply its endorsement, recommendation, or favoring by the United States Government or any agency thereof. The views and opinions of authors expressed herein do not necessarily state or reflect those of the United States Government or any agency thereof.

MASTER

DISTRIBUTION OF THIS DOCUMENT IS UNLIMITED

DISCLAIMER

This report was prepared as an account of work sponsored by an agency of the United States Government. Neither the United States Government nor any agency thereof, nor any of their employees, makes any warranty, express or implied, or assumes any legal liability or responsibility for the accuracy, completeness, or usefulness of any information, apparatus, product, or process disclosed, or represents that its use would not infringe privately owned rights. Reference herein to any specific commercial product, process, or service by trade name, trademark, manufacturer, or otherwise does not necessarily constitute or imply its endorsement, recommendation, or favoring by the United States Government or any agency thereof. The views and opinions of authors expressed herein do not necessarily state or reflect those of the United States Government or any agency thereof.

DISCLAIMER

Portions of this document may be illegible in electronic image products. Images are produced from the best available original document.

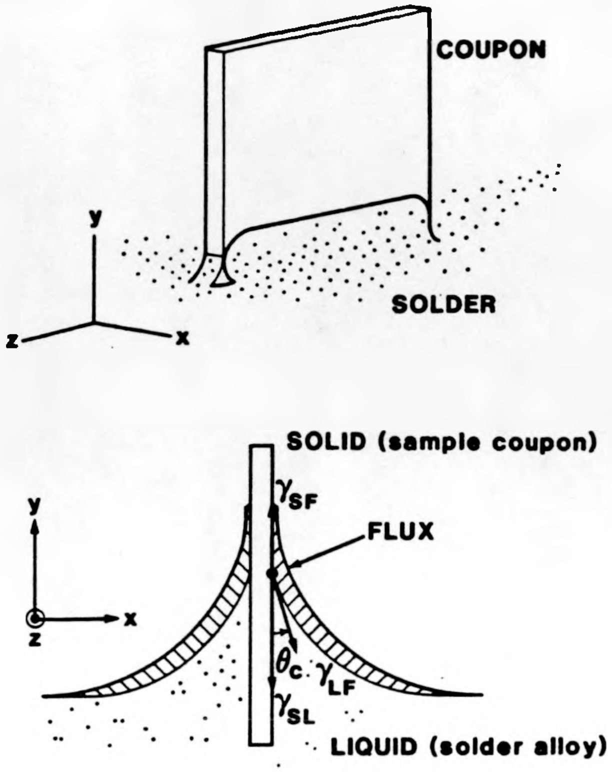

$$\gamma_{SF} - \gamma_{SL} = \gamma_{LF} \cos \theta_c$$

Fig. 1 – Schematic diagram of the sample test geometry and the application of Young's equation to the meniscus.

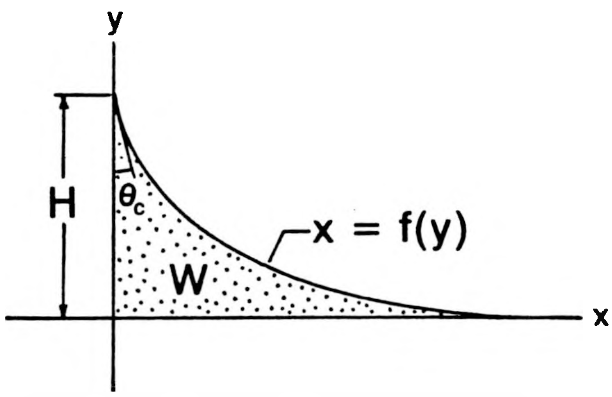

Fig. 2 – The meniscus properties used to calculate the wettability parameters.

The equations for θ_c and γ_{LF} are obtained by first considering the expression for the meniscus profile, $x(y)$, given by [5]:

$$x(y) = \sqrt{\frac{2\gamma_{LF}}{\rho g}} \left\{ \frac{1}{2\sqrt{2}} \ln\left[\frac{\sqrt{2}+q}{\sqrt{2}-q}\right] - \frac{1}{2\sqrt{2}} \ln\left[\frac{\sqrt{2}+q_c}{\sqrt{2}-q_c}\right] - q + q_c \right\} \quad (1)$$

where:

$$q = \sqrt{2 - \frac{\rho g y^2}{2\gamma_{LF}}} \quad , \quad q_c = \sqrt{2 - \frac{\rho g H^2}{2\gamma_{LF}}}$$

ρ is the density of the solder and g is the acceleration due to gravity. The meniscus weight is determined from the following equation [6]:

$$W = \rho g \, P \int_0^H x(y)\, dy = \rho g \, P \frac{H}{2} \sqrt{\frac{4\gamma_{LF}}{\rho g} - H^2} \quad (2)$$

where P is the perimeter of the coupon, and the cross sectional area of the meniscus is defined by the above integral. Because both W and H are experimentally measured quantities, the value of γ_{LF} can be solved from equation (2):

$$\gamma_{LF} = \frac{\rho g}{4}\left[\frac{4W^2}{(\rho g \, PH)^2} + H^2\right] \quad (3)$$

Furthermore, the relationship between the contact angle, the solder-flux interfacial tension, and the meniscus height can be shown to be:

$$1 - \sin \theta_c = \frac{\rho g H^2}{2\gamma_{LF}} \quad (4)$$

From equations (3) and (4), the contact angle can be expressed as a function of H and W by the following equation:

$$\theta_c = \sin^{-1}\left[\frac{4W^2 - (\rho g \, PH^2)^2}{4W^2 + (\rho g \, PH^2)^2}\right] \quad (5)$$

The determination of H and W was made by the meniscometer and wetting balance techniques, respectively (Fig. 3). The meniscometer (Fig. 3a) was a vertical traveling microscope capable of measuring the meniscus height to within an absolute error of ± 0.002 cm. The wetting balance system (Fig. 3b) was comprised of an electrobalance and a computer. The computer served to control the solder pot movement for immersion of the coupon into the solder as well as to acquire and analyze the meniscus weight signal from the balance. The absolute error of the meniscus weight measurement was ± 30 dynes.

Computation of the values of γ_{LF} and θ_c were performed as outlined in Fig. 4. Five coupons were tested on the meniscometer and five were analyzed on the wetting balance. The mean meniscus height, $\overline{H}$, and the mean meniscus weight, $\overline{W}$, were used to calculate $\overline{\gamma}_{LF}$ and $\overline{\theta}_c$. The minimum values of γ_{LF} and θ_c ($\gamma_{LF,min}$ and $\theta_{c,min}$, respectively) were calculated by using $\overline{H} + H_{1\sigma}$ and $\overline{W} - W_{1\sigma}$ in equations (3) and (5). Likewise, the maximum values of γ_{LF} and θ_c ($\gamma_{LF,max}$ and $\theta_{c,max}$, respectively) were determined by introducing $\overline{H} - H_{1\sigma}$ and $\overline{W} + W_{1\sigma}$ into the same two equations. The error terms, $\pm\theta_c$ and $\pm\gamma_{LF}$, were determined from the expressions:

$$\pm\theta_c = \pm\frac{(\theta_{c,max} - \theta_{c,min})}{2} \quad (6a)$$

$$\pm\gamma_{LF} = \pm\frac{(\gamma_{LF,max} - \gamma_{LF,min})}{2} \quad (6b)$$

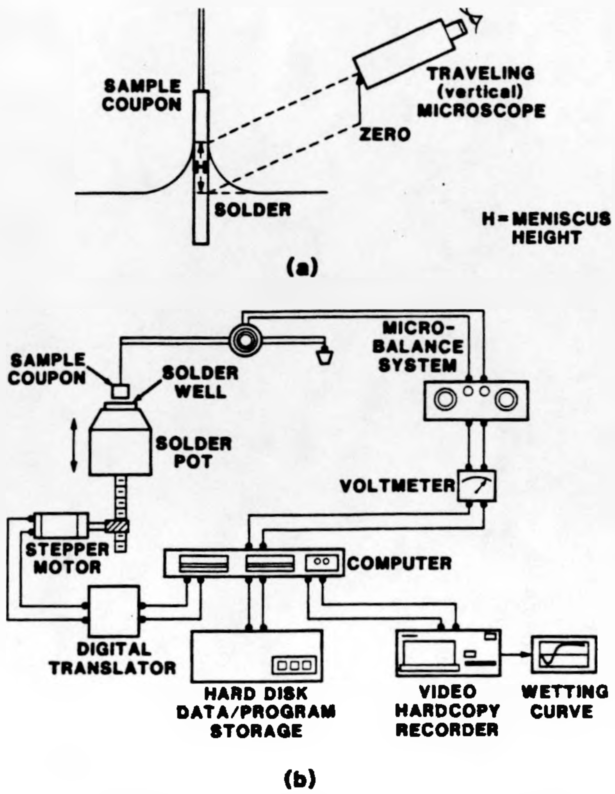

Fig. 3 – Schematic diagrams of (a) the meniscometer and (b) the wetting balance that determined the meniscus height and the meniscus weight, respectively.

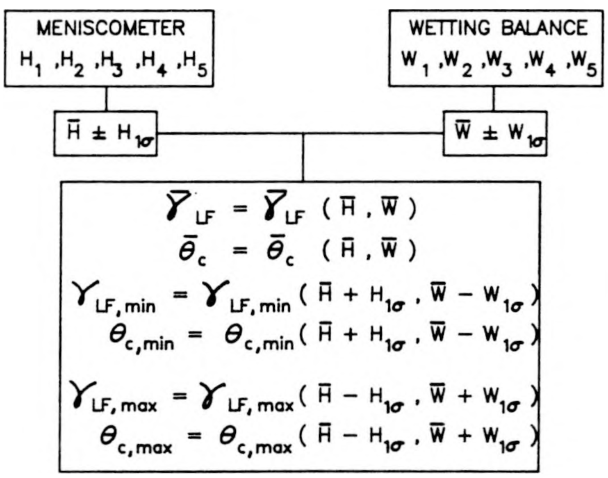

Fig. 4 – Outline of the steps used to calculate the mean contact angle, the mean solder-flux interfacial tension, and the ± error terms of each quantity.

The value of $(\gamma_{SF} - \gamma_{SL})$ was calculated from the product of γ_{LF} and cos θ_c. The error was determined from plus-or-minus the sum of the percent errors of $\pm\ \theta_c / \bar{\theta}_c$ and $\pm\ \gamma_{LF} / \bar{\gamma}_{LF}$ for θ_c and γ_{LF}, respectively.

The values of the wetting rate, $\dot{W}$, and the wetting time, t_W, were taken from the wetting curve of the meniscus weight, W, versus time, t (Fig. 5). The mean values were determined from the five wetting balance tests; the error terms were one standard deviation of each of the data sets.

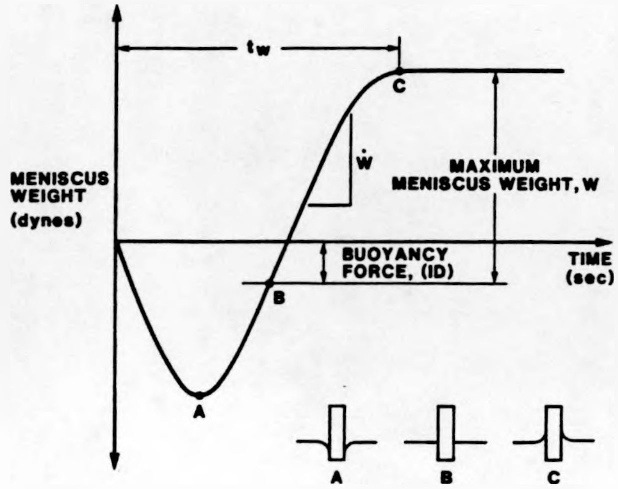

Fig. 5 – Representation of the generic wetting curve of meniscus height versus time measured by the wetting balance technique.

MATERIALS – The tin-rich, lead-free solders examined in this work were 95.5Sn-4.0Cu-0.5Ag, 95Sn-5Sb and 96.5Sn-3.5Ag. The 60Sn-40Pb alloy was added as a performance baseline. All materials were purchased from certified commercial sources. The working temperatures of the solders were 267°C for 95.5Sn-4.0Cu-0.5Ag, 280°C for 95Sn-5Sb, 260°C for 96.5Sn-3.5Ag, and 260°C for 60Sn-40Pb.

The substrates were oxygen-free, high conductivity (OFHC) copper coupons measuring 2.54 × 2.54 × 0.0254 cm. The coupons were cut from rolled stock and retained the as-rolled surface finish. Each copper sample was degreased in an agitated bath of trichlorethylene followed with an isopropyl alcohol rinse. Next, the specimen was etched in a bath of 1:1 hydrochloric acid and deionized water. The samples were then rinsed in water and isopropyl alcohol. The specimens were coated with flux immediately after completion of the cleaning procedure.

The fluxes used in this study were (1) Alpha 611™, RMA [7]; (2) Alpha 250HF™, OA (alcohol-based); (3) Alpha 260HF™, OA (alcohol-based); and (4) Blackstone 2508™, OA (water-based) [8]. The particular brands of flux were selected for their range of activities as observed in previous use; this is not to be construed as a product endorsement. The fluxes were diluted 1:1 with isopropyl alcohol and designated as A611, A250HF, A260HF, and B2508, respectively.

RESULTS AND DISCUSSION

Shown in Fig. 6 are the contact angle data as a function of flux and the particular solder alloy. The solder alloys 95Sn-5Sb and 95.5Sn-4.0Cu-0.5Ag exhibited non-wetting of the substrate coated with the A250HF flux; the contact angles were designated 180° in those cases. The 95Sn-5Sb and 95.5Sn-4.0Cu-0.5Ag solders exhibited mean contact angles of 46° to 51° and 34° to 48°, respectively, for each of the three fluxes A611, A260HF, and B2508. The 96.5Sn-3.5Ag solder showed higher mean contact angles of 58° to 62° for the same fluxes. Unlike the other lead-free solders, the

96.5Sn-3.5Ag alloy did exhibit wetting with the A250HF flux; however, the mean contact angle was very high at a value of 78°. The control alloy, 60Sn-40Pb, exhibited the anticipated lower contact angles of 23° to 35° for all four fluxes. For the 95Sn-5Sb, 95.5Sn-4.0Cu-0.5Ag and 60Sn-40Pb solder alloys, no statistically significant trend was observed in the contact angle data as a function of the fluxes A611, A260HF, and B2508. The only appreciable difference was observed with the A250HF flux and the lead-free solders in which wetting deteriorated. In summary, the wettability of the lead-free solders 95Sn-5Sb and 95.5Sn-4.0Cu-0.5Ag was "fair to good" in comparison to the "excellent" wetting of the 60Sn-40Pb solder, thereby allowing these alloys to be candidates for replacement of the control solder.

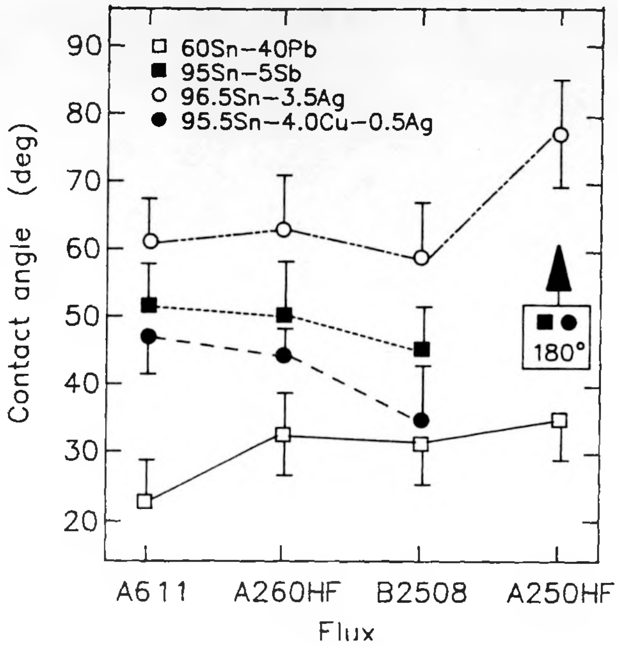

Fig. 6 – Contact angle as a function of flux and solder type.

The values of γ_{LF} and $(\gamma_{SF} - \gamma_{SL})$ were examined for insight into the wetting conditions affecting the contact angle values. Shown in Fig. 7 is a plot of the solder-flux interfacial tension, γ_{LF}, as a function of flux type and solder. The values of γ_{LF} were similar for the solders 95Sn-5Sb (650 dyne/cm) and 95.5Sn-4.0Cu-0.5Ag (660 dyne/cm) with use of the RMA flux. These values were higher than that of the 60Sn-40Pb solder (460 dyne/cm). The values of γ_{LF} from each of these three solders were similar for the A260HF and B2508 fluxes. Finally, the values of γ_{LF} for the 96.5Sn-3.5Ag solder were markedly higher, including a value of 3850 dyne/cm with the A250HF flux.

The $(\gamma_{SF} - \gamma_{SL})$ results are presented in Fig. 8. For all three fluxes, A611, A260HF, and B2508, the values were very similar for the 95Sn-5Sb and 95.5Sn-4.0Cu-0.5Ag solders. The 60Sn-40Pb control had nearly the same value of $(\gamma_{SF} - \gamma_{SL})$ as the two lead-free solders with the RMA flux only; otherwise, the values were slightly larger.

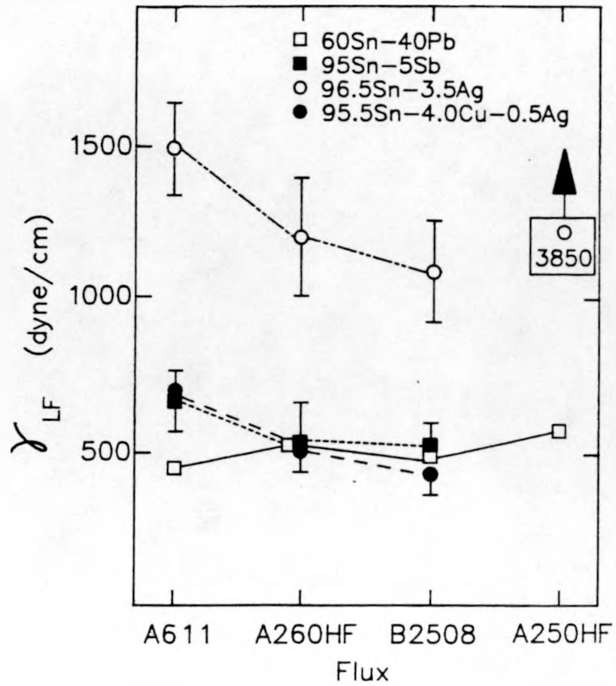

Fig. 7 – Solder-flux interfacial tension as a function of flux and solder type.

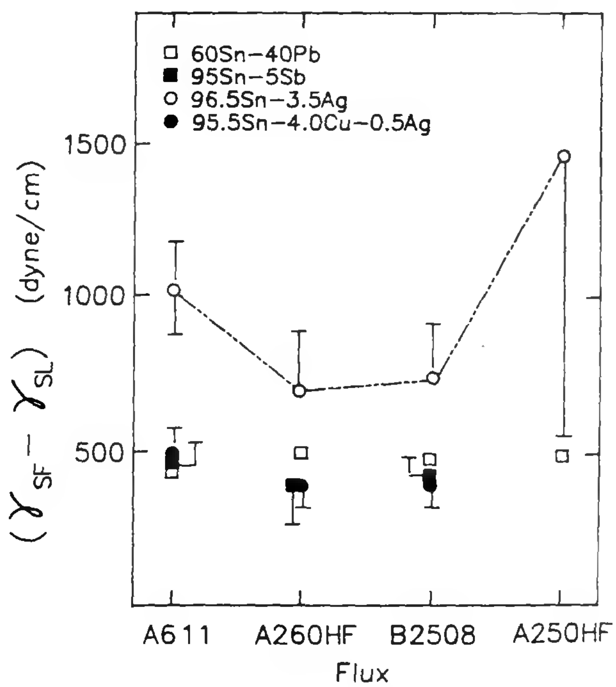

Fig. 8 – $(\gamma_{SF} - \gamma_{SL})$ as a function of flux and solder type.

A physical interpretation of the γ_{LF} and $(\gamma_{SF} - \gamma_{SL})$ data provides information as to the controlling factor in the value of the contact angle. Generally, the lead-free solders 95Sn-5Sb and 95.5Sn-4.0Cu-0.5Ag exhibited similar wetting behaviors. A slightly lower θ_c was recorded with the 95.5Sn-4.0Cu-0.5Ag solder and B2508 flux due to a slight reduction in γ_{LF}. A611 was more effective at lowering the solder-flux interfacial tension of the 60Sn-40Pb solder than the values of the lead-free solders. The OA fluxes A260HF and B2508 caused little difference in γ_{LF} between 95Sn-5Sb, 95.5Sn-4.0Cu-0.5Ag, and 60Sn-40Pb. These results indicate that the attribute of adding lead to tin to lower the solder surface tension was not always realized; rather, the value of γ_{LF} can be as strong a function of the flux as of the solder alloy composition. The 96.5Sn-3.5Ag solder provided evidence of the effect of solder composition (3% silver) on the interfacial tension, irrespective of the composition of the flux. These results clearly demonstrate the absolute necessity of wettability testing to evaluate the *combined* solder-substrate-flux system.

The $(\gamma_{SF} - \gamma_{SL})$ data (Fig. 8) provided information about metallurgical interactions at the solder-substrate interface. Use of a single flux infers that γ_{SF} remains constant. Therefore, the term $(\gamma_{SF} - \gamma_{SL})$ from Young's equation reflects the behavior of γ_{SL}. For each of the fluxes A611, A260HF, and B2508, the two lead-free solders 95Sn-5Sb and 95.5Sn-4.0Cu-0.5Ag exhibited nearly identical values of $(\gamma_{SF} - \gamma_{SL})$. Similar data for the 60Sn-40Pb solder were at most only slightly different for the particular fluxes examined. These observations indicated that in spite of the composition difference between the two solders, their solder-substrate interfaces, which are more accurately described as the interface between the solder and the intermetallic layer arising from the reaction between the Sn in the solder and the copper substrates (Fig. 9), had the same wetting properties. It was also clear from Fig. 9 that although the intermetallic layers showed similar wettability, their physical morphology was sensitive to the solder composition.

The $(\gamma_{SF} - \gamma_{SL})$ values from the 96.5Sn-3.5Ag solder exceeded the those from the other solders for each of the fluxes. Apparently, the relatively high concentration of silver enhanced those alloy reactions at the solder-substrate interface which caused a substantial decrease to γ_{SL}.

For the most part, the values of $(\gamma_{SF} - \gamma_{SL})$ for all of the solders (excluding the 96.5Sn-3.5Ag alloy) and the fluxes (excluding A250HF) were within a range of only 100 dyne/cm. This observation, coupled with similar wettability at the solder-substrate interface (i.e., similar γ_{SL}), implies that γ_{SF} was not dramatically different, in spite of the range of activities expected between the relatively weak RMA and the stronger OA fluxes. A likely reason for this behavior was that the extensive pre-cleaning procedures used on the copper substrate limited the oxide thickness requiring reduction, so that the RMA flux was more than adequate to promote wetting; the added strength of the OA fluxes was not necessary.

Overexposure of the substrates to those temperatures necessary to reflow the solder can cause degradation to the substrate and the flux ("charring"), re-oxidation of the solder and substrates, and damage to components. These points are especially critical to manual (hand) soldering process. Typical soldering iron tip temperatures are 400°C to 480°C. Prolonged contact between the iron and the bonding pad can cause permanent damage to the underlying substrate, causing the pad layer to lift off. Shown in Figs. 10 and 11 are the wetting rate ($\dot{W}$) and the wetting time (t_W) data, respectively, measured from the wetting balance plots. No significant differences for either $\dot{W}$ or t_W were observed between 95.5Sn-4.0Cu-0.5Ag, 95Sn-5Sb, and the control solder, 60Sn-40Pb, with any of the fluxes. This observation indicates (to a first order) that the time required to form joints will be similar with all three solders. Processing with the 96.5Sn-3.5Ag solder will be more difficult due to the slower rate of wetting. However, it should be understood that the wetting rate will also be dependent upon the geometry of the particular joint. For example, open configurations such as edge clips can show expeditious wetting, even with the use of the 96.5Sn-3.5Ag solder [1]. On the other hand, the same solder may show sluggish wetting of confined geometries, such as through-holes, because of its very high surface tension.

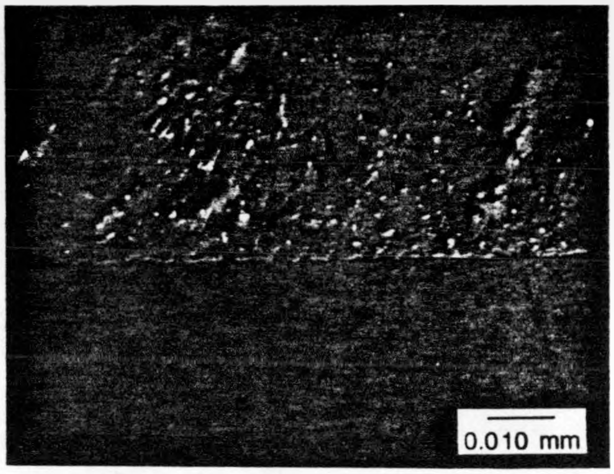

(a)

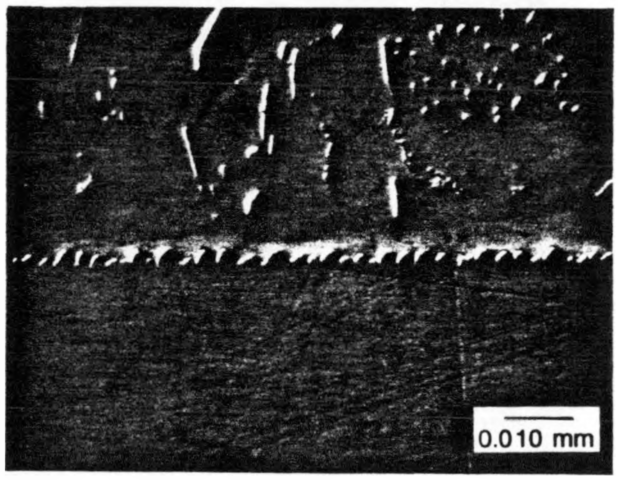

(b)

Fig. 9 – Optical micrographs of the intermetallic layer formed at (a) the solder-substrate interface of the 95Sn-5Sb solder and (b) the 95.5Sn-4.0Cu-0.5Ag solder. In each case, the copper substrate is at the bottom of the picture.

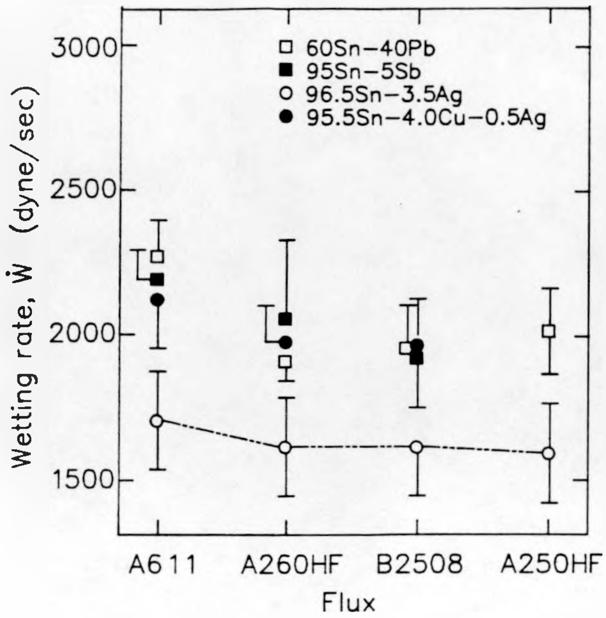

Fig. 10 – Wetting rate data as a function of flux and solder alloy.

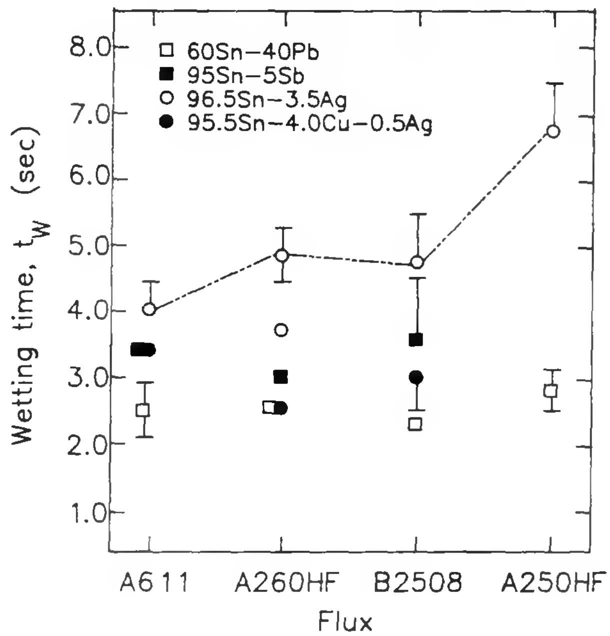

Fig. 11 – Wetting time data as a function of flux and solder.

A qualitative assessment was made of the solder films formed on the copper substrates. The 95Sn-5Sb and 96.5Sn-3.5Ag alloys exhibited smooth, shiny solder films not unlike those of the 60Sn-40Pb material. The 95.5Sn-4.0Cu-0.5Ag solder had a very grainy appearance. The rough topography was caused by the suspension of Cu_xSn_{1-x} intermetallic compound crystals, which formed from the Cu and Sn constituents in the solder, and tin-silver intermetallic particles. Shown in Fig. 12 are optical micrographs of the 95.5Sn-4.0Cu-0.5Ag solder film (a) on a wetting balance test coupon and (b) on a thicker film on a copper substrate. The Cu_xSn_{1-x} crystals were prevalent within the solder bulk. The presence of the intermetallic crystals would not likely affect the wetting behavior of the solder in an open geometry such as that encountered in pretinning operations (which the wetting test most closely resembles). However, in more confined geometries such as pin-in-hole joints, capillary flow may become restricted or be blocked altogether by the particles.

Finally, one sample coupon was selected from each test series and thoroughly cleaned immediately after withdrawal from the solder pot. Samples coated with the RMA flux were cleaned in trichloroethylene, de-ionized water, and isopropyl alcohol. The organic acid flux residues were removed by rinsing in hot tap water, de-ionized water, and isopropyl alcohol. Each sample was then examined to determine the extent of flux residues formed on the coupon surface. It must be kept in mind that, although the individual solder temperatures represented likely values for actual processing conditions found in both manual and automated soldering operations, the hold time of 20 seconds exceeds typical process time periods at those temperatures. Nevertheless, a relative performance can be developed from the specimens, although the test conditions were more severe than those found in normal practice.

All of the organic acid fluxes left some brown/black residues, the extent of which varied between the various materials. Residues were lightest with the A260HF flux and relatively heavy with the B2508 and A250HF solutions. The residues were most severe with the 95Sn-5Sb solder due to the 280°C working temperature. Tan residues were also observed with the A611 RMA flux. Only the B2508 flux showed an extent of flux residue that was dependent upon the solder alloy (exclusive of 95Sn-5Sb). The B2508 residue was heaviest on the 95.5Sn-4.0Cu-0.5Ag and lightest for 60Sn-40Pb and 96.5Sn-3.5Ag.

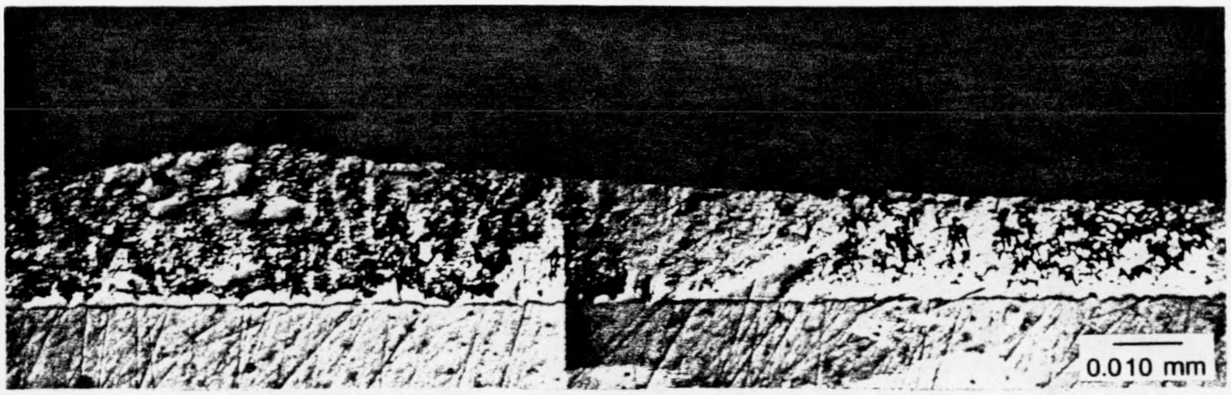

(a)

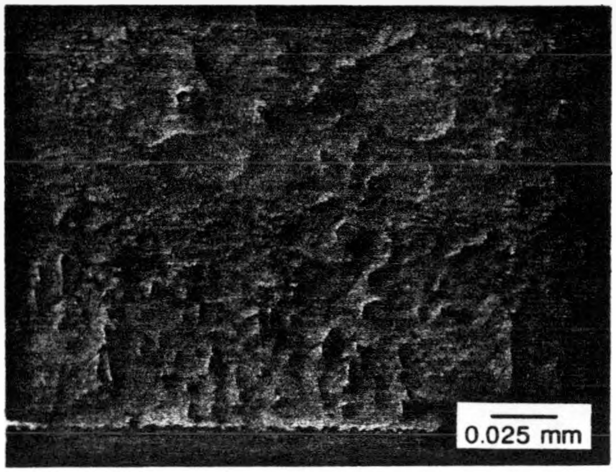

(b)

Fig. 12 – Optical micrographs of the thin 95.5Sn-4.0Cu-0.5Ag solder film (a) on a wetting balance sample and (b) a thicker solder film also on a copper substrate. For both micrographs, the copper substrate is at the bottom of the picture.

CONCLUSIONS

1. The tin-rich, lead-free solders 95.5Sn-4.0Cu-0.5Ag and 95Sn-5Sb exhibited "fair to good" wetting ($34° < \theta_c < 51°$) on copper with the RMA flux, A611, and the organic acid fluxes, A260HF and B2508. These results are compared to the "excellent" wetting ($20° < \theta_c < 35°$) observed by the control solder, 60Sn-40Pb. Nevertheless, the performance of the tin-rich solders would allow them to be suitable alternatives for the 60Sn-40Pb alloy.
2. The tin-rich solder, 96.5Sn-3.5Ag, exhibited only fair wettability ($60° < \theta_c < 75°$). The poor performance as compared to the control solder was due largely to the higher value of γ_{LF} accompanying the solder.
3. The wetting rates and wetting times of the 95Sn-5Sb and 95.5Sn-4.0Cu-0.5Ag solders were comparable to values from the 60Sn-40Pb solder. The wetting rates and wetting times were slower and longer, respectively, for the 96.5Sn-3.5Ag solder than any of the other alloys.
4. Smooth, shiny, uniformly thick solder films were obtained with the 96.5Sn-3.5Ag and 95Sn-5Sb. The 95.5Sn-4.0Cu-0.5Ag solder films had a very grainy morphology caused by the presence of Cu-Sn intermetallic crystals in the tin matrix.
5. The residues left by the organic acid fluxes were more extensive and tenacious than those from the RMA flux after 20 seconds of exposure to the solder working temperatures.

ACKNOWLEDGMENT

This work was performed by Sandia National Laboratories for the United States Department of Energy under Contract DE-AC04-76DP00789.

REFERENCES

[1] Vianco, P. and J. Dal Porto, "Use of High Temperature Solders for Edge Clip Attachment on Polyimide-Quartz Circuit Boards", *Proc. Third Elec. Mat. and Proc. Congress*, Aug. 1990, San Francisco, CA, p. 25.

[2] Engelhard Corp., Mansfield, Mass.

[3] Manko, H., *Solders and Soldering*, 2nd Ed., (NY; McGraw-Hill 1979) p. 48.

[4] Montreal Protocol Agreement, 1990.

[5] Mayhew, A., and K. Monger, "Solderability by Meniscometry", *Proc. Inter. NEPCON IV*, (1972) p. 53.

[6] Vianco, P., F. Hosking, and J. Rejent, "Solderability Testing of Kovar with 60Sn-40Pb Solder and Organic Fluxes", *Weld. J.*, (June 1990), p. 230s.

[7] Alpha Metals, Jersey City, NJ.

[8] Blackstone Corp., Jamestown, NY.